

## Study on the Design and Control of Pipeline Leak Detection Robot Fish

*Jian-xian Cai, Xu Zhou, Zhen-ling Pan, Peng-gang Gao, Yu-xin Luo, Zi-xian Lin*

*Department of Disaster Prevention Instrument, Institute of Disaster Prevention, Yanjiao Development Zone, Sanhe, Hebei Province, 065201, China  
E-mail: cjxlaq@163.com*

**Abstract:** *Based on the simplified fish motion model, a robot fish which could detect the oil leakage point of pipeline was designed by the method of single-joint driving. The Hawkeye OV7725 was used to design the image acquisition module to obtain the current movement of the fish and the current pipeline situation and the collected data was processed for making the relevant decisions to achieve the direction of movement control with the STM32 microcontroller. On the basis of binarization image centroid method, the image recognition algorithm was studied. By using the coordinates of the white point in the two-dimensional array, a linear regression equation which can reflect the distribution trend of the white point in a frame image was designed and the motion direction of the current robot could be detected. Since the linear regression equation converge to the characteristics of discrete data points, the oil leakage point inside the white area of the image could be detected. Experiment results showed that the robot fish can effectively complete the oil spill point detection task.*

**Keywords:** *Robot fish, image acquisition, binarization, linear regression.*

### 1. Introduction

With the progress of society and the development of science and technology, the demand of human being for oil increases day by day. The exploitation of oil from all over the world has extended from inland to coastal areas even deep sea. With the increase of offshore oil and gas fields, oil pipelines have been distributed vertically and horizontally in the seabed like blood vessels, shouldering the mission of transporting this black industrial blood. The following monitor on the leak of oil pipeline has become unavoidable problem for each country.

The main factor that affect the safety of submarine pipelines is corrosion. Nowadays, the common pipeline inspection method [1-5] is divided into the following three types: Manual sampling method, positioning and key node detection method and waterborne robot inspection method. Manual sampling method achieves

pipeline inspection by human source with high locating accuracy. However, this method cannot fully detect the submarine pipeline, and it is labor-intensive and costly. The method of positioning and key node detection is based on electronic sensor applied both inside and outside of the pipeline. For instance, odor sensor determines whether the pipeline leaks by detecting the smell of oil, but this method can only apply inspection on local points, and it wears easily in water. As robot technology develops rapidly, underwater vehicle has become the most advanced underwater detection equipment all over the world. It plays a significant role in promoting the development of submarine pipeline detection. Z e h u i J i [6], student of Ocean University of China, proposed an inspection method based on submarine pipeline corrosion, using the surrounding electric field distortion theory. The corrosion is inspected by the measurement of submarine pipeline through the magnetic exploration system, potentiometric sensor system and other sensors that are carried by the robot. However, each module of this method only has single function, set up devices will be too much, resulting in occupying a large number of hardware resources and higher cost.

In conclusion, most of current pipeline detection methods needs large amount of machines and have high cost due to adoption of non-visual sensors. In addition, the current methods that work by the underwater robot equipped with sensors mostly focused on detection and ignore the pipeline tracing research, lacking autonomy.

As a result, it is necessary to explore a low cost, independent and efficient method for detecting oil spills. This article will start with convenience, efficiency, and low-cost to design a simple single joint robot fish with image acquisition based on binarization [7-10] camera and design the algorithm of tracing and oil leaking point detect by Linear regression equation.

## 2. Design of hardware

### 2.1. Operating principle

In Fig. 1, binarization camera is used for image acquisition, STM32 chip is used for image procession and the alarm system consists of buzzer and LED lights. In addition, the power of STM32 microcontroller and LED fill light system are supplied by two sets of lithium batteries respectively. STM32 microcontroller processes collected data and make relevant decision on the s3102 servo output control signals to achieve control of movement direction.

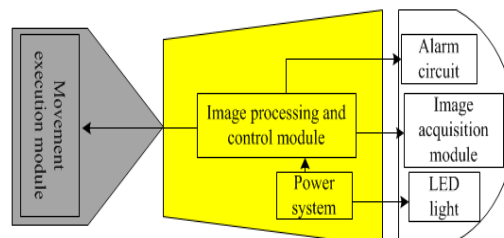


Fig. 1. Hardware construction of robot fish

## 2.2. Image acquisition

Due to high signal-to-noise ratio, high acquisition speed, good stability, high low-light sensitivity Hawkeye OV7725 camera was adopted. Besides, the camera is compatible with SCCB protocol and integrates logic chip to capture high-speed images and output high quality binary images which is transported to STM32 for processing through eight GPIOs channel.

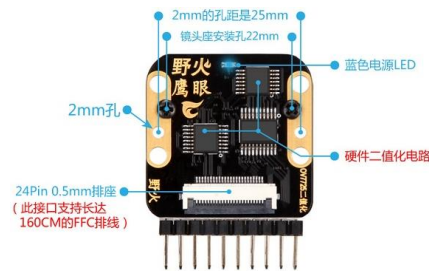


Fig. 2. Hawkeye OV7725

## 2.3. Image processing and control

In this module, STM32 chip was adopted for its abundance in resources and high processing speed. There are two main functions of STM32 chip. First, the chip could receive and analyze the data collected by Hawkeye OV7725 camera and initialize the camera (i.e., set a threshold value). The other one is achieving control signal based on processed data and sending the signal to servo through GPIO channel. The servo is type S3102.



Fig. 3. STM32 chip



Fig. 4. Servo S3102

Two sets of lithium battery are used in the power system to supply electricity for image processing and LED light individually. Moreover, an easy alarm circuit was designed to assist prompts whether an oil leak has been detected. This circuit mainly use the switching characteristic of bipolar transistor for connecting buzzer and LED lights to realize the alarm.

## 3. Algorithm design

### 3.1. White pipe tracing algorithm design

In the process of pipe tracing, binarization threshold parameter of the camera is adjusted by software. The pipe is represented by 1 and 0 is on behalf of water. As is shown in the Fig. 5, the white area in the middle represents pipes and the black area on the two sides are water. This picture is an ideal model.



Fig. 5. Pipe model

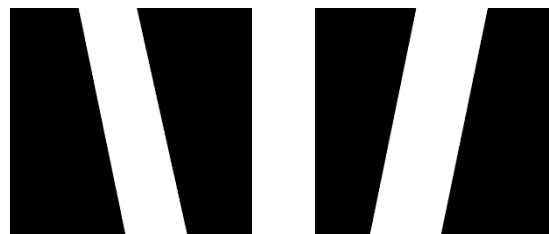
The feedback images are divided into the following simple models by Visio drawing tools, as is shown in Figs 6 and 7.



(a) Left-deflected

(b) Right-deflected

Fig. 6. Horizontal deflection model



(a) Left-deflected

(b) Right-deflected

Fig. 7. Oblique deflection model

In the pictures above, Fig. 6 is horizontal deflection model, Fig.7 is oblique deflection model. As a result, the several following condition can be obtained by combining exceptions. The results are shown in the Table 1.

The speed and direction of the robot fish were represented by speed and direct respectively and they are all set for 15 levels. The fish stops moving when the speed=0, and the fish moves in the highest speed when the speed=15. When direct=7, the fish moves in the middle. And the fish moves to the left when  $0 < \text{direct} < 7$ . The fish moves to the right when  $7 < \text{direct} < 15$ .

Table 1. Combination of moving situation

Horizontal displacement	Angle of inclination (°)	Condition of robot fish
$\Delta x = 0$	$\theta = 90$	Fish body along pipeline and move straightly
$\Delta x = 0$	$\theta < 90$	Fish body along pipeline, head to the right
$\Delta x = 0$	$\theta > 90$	Fish body along pipeline, head to the right
$\Delta x < 0$	$\theta = 90$	Fish body on the left, head along the pipeline
$\Delta x < 0$	$\theta < 90$	Fish body on the left, head to the right
$\Delta x < 0$	$\theta > 90$	Fish body on the left, head to the left
$\Delta x > 0$	$\theta = 90$	Fish body on the right, head along the pipeline
$\Delta x > 0$	$\theta < 90$	Fish body on the right, head to the right
$\Delta x > 0$	$\theta > 90$	Fish body on the right, head to the left

To make sure the robotic fish can recover rapidly from abnormal situation and keep moving along the pipeline, the following relation is used:

$$(1) \quad \text{direct} = C \times (A \times k + B \times \Delta x) + 7,$$

where:  $A$  is the slope factor,  
 $B$  is the coefficient of horizontal displacement,  
 $C$  is the gain coefficient,  
 $k$  is the slope of the white pipe,  
 $\Delta x$  is the horizontal displacement.

### 3.1.1. Calculation of white pipe slope

According to the coordinates of the white pixels of each image captured, a linear regression equation [11-13]  $y = \hat{a} + \hat{b}x$  can be applied for calculation.  $\hat{a}$  and  $\hat{b}$  are regression coefficient. The expressions of the parameters are shown as follow:

$$(2) \quad \hat{b} = \frac{\sum_i^n x_i y_i - n \bar{x} \bar{y}}{\sum_i^n x_i^2 - n \bar{x}^2},$$

$$(3) \quad \hat{a} = \bar{y} - \hat{b} \bar{x},$$

where:  $k = \hat{b}$  represents the slope of the white pipe,  
 $x_i$  is the horizontal coordinate of the sample values,  
 $y_i$  is the vertical coordinate of the sample values,  
 $\bar{x}$  is the average value of the horizontal coordinate of the sample values,  
 $\bar{y}$  is the average value of the vertical coordinate of the sample values,  
 $n$  is the number of sample values.

### 3.1.2. Calculation of horizontal displacement

( $\Delta x$ ): By analyzing the centroid horizontal position ( $x_c, y_c$ ) and original point of fixed coordinate system ( $x_0, y_0$ ), the horizontal displacement can be calculated, just like it is shown in Fig. 8.

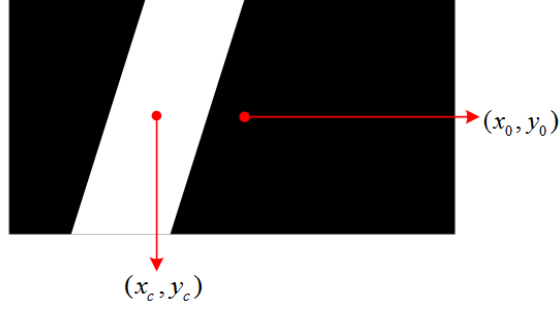


Fig. 8. Centroid model

Firstly, according to the centroid method introduced in [14], the centroid can be figured out as

$$(4) \quad (x_c, y_c) = \left( \frac{\sum_{ij} x_{ij} \times I_{ij}}{\sum_{ij} I_{ij}}, \frac{\sum_{ij} y_{ij} \times I_{ij}}{\sum_{ij} I_{ij}} \right),$$

where  $I_{ij}$  is the pixel lightness, ( $x_c, y_c$ ) is the coordinate of centroid,  $x_{ij}$  is the horizontal coordinate of the white pixels in row  $i$  and column  $j$ ,  $y_{ij}$  is the vertical coordinate of the white pixel in row  $i$  and column  $j$ .

In this equation,  $I_{ij}$  represents the lightness of the pixel in row  $i$  and column  $j$ . As a result, the horizontal deflection is

$$(5) \quad \Delta x = x_c - x_0.$$

### 3.1.3. Design of turn-off algorithm

When the first  $L$  (normally  $L \geq 3$ ) lines of the detected image are black (seen in Fig. 9), i.e., the first  $L$  rows of the feedback data matrix are 0, as shown in the next equation, then a flag was set to enter the turn program:

$$(6) \quad \begin{bmatrix} 0 & 0 & 0 & 0 \\ 1 & 1 & 1 & 0 \\ 1 & 1 & 1 & 0 \\ 0 & 1 & 1 & 0 \end{bmatrix}.$$



Fig. 9. Turn-off model

### 3.2. Design of black dots recognition

Ideally, the linear regression curve converges to the inside of the white pipe. However, due to the actual interference of the outside world, there will be three major exceptions, as shown in Fig. 10.

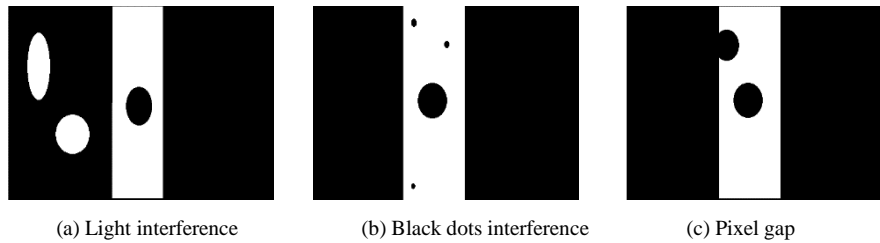


Fig. 10. Interference model of oil leaking point

The abnormal situation in Fig. 10a is that large white spots will appear on the image because of light and other reasons. To deal with such situation, the vertical distance of white dots to linear regression equation ( $d$ ) is calculated firstly then the variance  $\sigma$  of  $d$ . When the variance is bigger than certain threshold value, this frame of image is taken as effective image. Otherwise, the image is abandoned and next frame of image is taken.

The abnormal situation in Fig. 10b is that the white area of each frame will appear fragmented pixel bubble interference point when the voltage is not stable. In this situation, the radius ( $r$ ) of the black dots are calculated and the limitation is given. When  $r$  is larger than certain threshold value, this black dot will be taken as oil leaking point.

The abnormal situation in Fig. 10c is that pixel gap appears in the white areas in every frame of image when the voltage is unstable. Under this circumstance, a limiting condition is set. Only when the number of white pixel per line is bigger than certain threshold, this frame of image is taken as effective one. Otherwise this picture is abandoned and next frame of images was taken.

After removal of interference, the black pixels are searched inside the white area along the linear regression curve (i.e., find pixels with the code value of 0). When the pixels are more than certain numbers, the establishment of signs will be done to prompt CPU that oil leaking point was detected. Then the sign is detected and fed back to the host computer by alarm program module to drive the alarm circuit.

The specific algorithm flow chart is shown in Fig. 11. The collected images are stored in the array space in the form of binary code. According to scan result of the previous lines to find out whether they were 0, whether there was a turn-off corner can be determined. The following process is the oil spill point recognition program to determine whether there was oil spill point. If so, the alarm is triggered. Otherwise, correct the direction of movement.

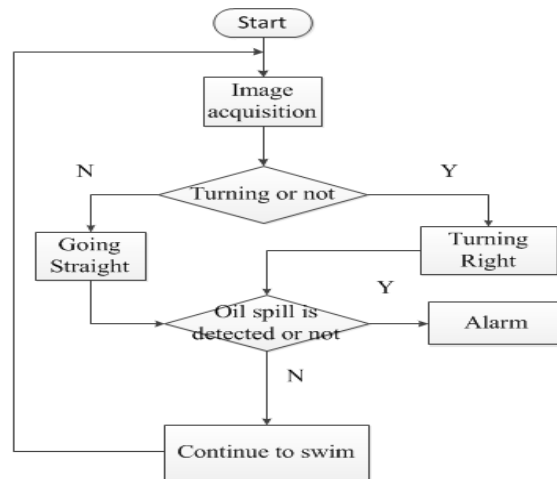


Fig. 11. Flow chart of algorithm

## 4. Experiment and data analysis

### 4.1. Experiment environment and setting

The PVC tube with diameter of 75 mm was put in the bottom of the pool to simulate the oil pipeline. Oil spots were marked by black solid circle with the diameter of 3 cm. Eight oil leaking points were set and randomly distributed throughout the pipeline. The experimental scene overlooking model is shown in Fig. 12. During the experiment, the fish began at the starting point shown in the figure, cruised along the white pipeline, passed through two corners, swam to the end. During this process, the alarm system would be triggered if the black oil spilling points were detected.

Experiment parameter setting is as follow.

Lines without whit pixels  $L=3$ , threshold value of variance  $\zeta_1=10$ , threshold value of radius of black dots  $\zeta_2=5$ , threshold value of number of white pixels per line  $\zeta_3=15$ . The parameter setting in Equation (1) are as follow:  $A=12$ ,  $B=4$ ,  $C=7$ . The value of these parameters were adjusted during the experiment.



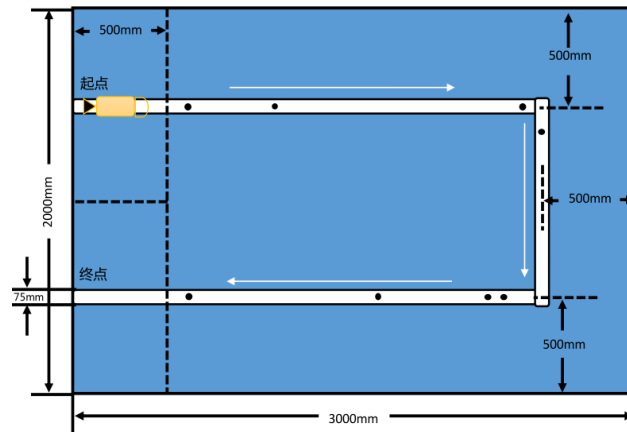


Fig. 12. Experimental scene overlooking model

#### 4.2. Result and analysis

Firstly, the value of  $A$ ,  $B$  and  $C$  in equation (1) were determined through experiment. Figs 14-16 shows the results of the difference ( $\Delta x$ ) between practical movement track and expected one.

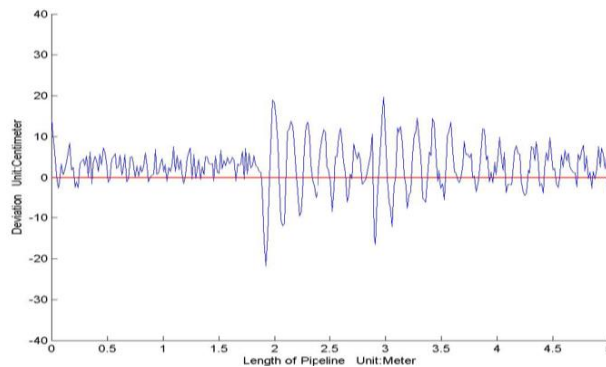


Fig. 13. Deviation curve ( $A=12$ ,  $B=4$ ,  $C=7$ )

As is shown in Fig. 13, the trajectory of robot fish cannot converge in the center of the white pipe, deviated from the heading with a large deviation level. The maximum deviation is 10 cm. Moreover, a large peak appeared in the turning period, which to some degree affected the trail quality of robot fish.

The deviation of the robot fish from the heading problem was promoted firstly. From Equation (1), heading direction was mainly affected by slope parameter  $A$ . During the experiment, it could be found that reduction in the value of  $A$  helped robot fish convergence to the desired heading motion. In Fig. 14,  $A=9$  and  $C=7.2$  correspondingly (not change simulation result of horizontal deviation coefficient). It is obvious from the result that the robot fish running essentially along the pipe center and the peak decreased at corners. However, the level deviation of robot fish is still large.

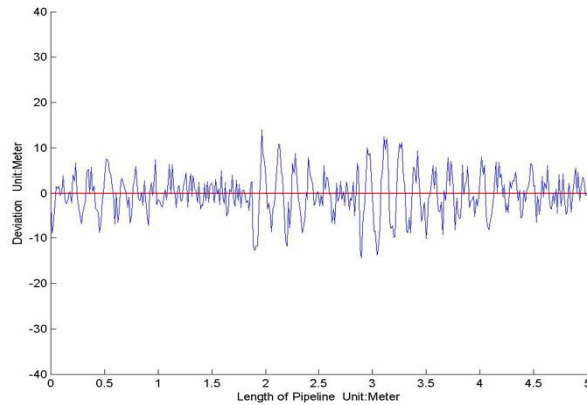


Fig. 14. Deviation curve ( $A=9, B=4, C=7.2$ )

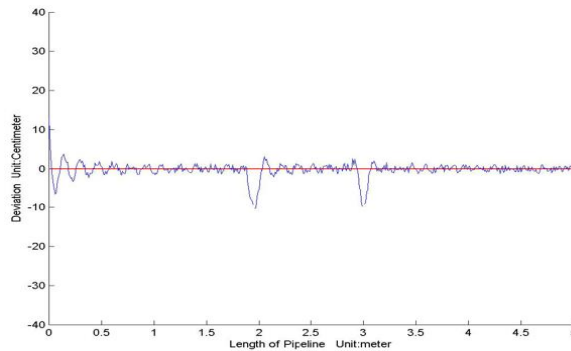


Fig. 15. Deviation curve ( $A=9, B=2, C=7.5$ )

As is known from Equation (1), parameter  $B$  mainly affects horizontal deviation. It was found during experiment that decreasing the value of  $B$  will reduce horizontal deviation, making the fish operate with low swing. In Fig. 15,  $B=2$  and  $C=7.5$  correspondingly. As is shown in the result, the deviation during straight moving reduced obviously and was controlled within 3 cm. What's more, the peak in the corner was improved obviously and the fish could run along the set course.

#### 4.3. Error analysis

During the experiment, when the fluorescent light irradiated the water surface, i.e., the situation in Fig. 10. the probability of the robot fish missing the oil leak point increases due to light interference. The nearest black oil leak point can't be detected. By adopting this anti-jamming algorithm, the robot fish is less likely to be interfered by light and can detect eight leaking point.

When the voltage is low, pixel gap and pixel bubbles would appear on the image, i.e., the situation shown in Fig. 10b and Fig. 10c, the probability of false oil leaking point report increases. When the voltage is less than 15%, it will miss report 1-3 leaking points. After algorithmic removal of interference, the robot fish could recognize eight oil leaking point without miss reporting.

#### 4.4. Physical experiment

In order to further verify the effectiveness of this design, the moving track of robot fish tracing along the pipe was taken. It is shown in Fig. 16. Compared with Fig. 15, it is obvious that the robot fish adopting designed algorithmic could operate along the set course, the same as simulation result.

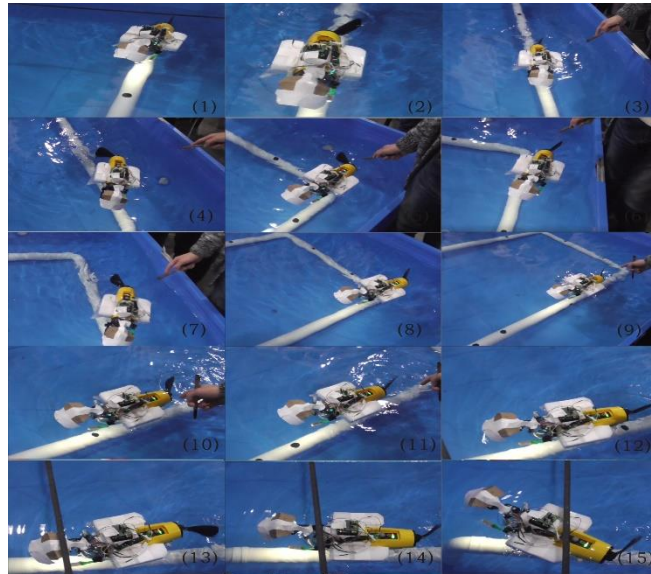


Fig. 16. Process of pipeline oil spill point detection

#### 5. Conclusion

In this article, based on the simplified fish motion model a robot fish which could detect the oil leakage point of pipeline only through binary camera was designed by the method of single-joint driving which has low cost. According to the need of applying environment, a linear regression equation which can reflect its distribution trend in on frame image was designed by using the coordinates of the white point in a two-dimensional array to detect current moving direction of robot fish. Since the linear regression equation converge to the characteristics of discrete data points, the oil leakage point inside the white area of the image could be detected.

In simulation and physical experiment, the process of pipeline oil spill point detection was simulated for different situations. The achievement was applied in practical robot fish pipeline inspection mission. The result showed that the tracing and recognition algorithm based on the Theory of Liner Regression Equation could help the robot fish finish oil leaking point detection while tracing in the pipeline and give the fish autonomy.

**Acknowledgments:** The work was supported by Scientific Research Plan Projects for Higher Schools in Hebei Province (No ZD2018304); Special Fund of Fundamental Scientific Research Business Expense for Higher School of Central Government (Project for creation teams No ZY20180111).

## References

1. Wang, Z. A New Method of Pipeline Leak Detection. – China Measurement & Test, Vol. **42**, 2015, No 5, pp. 31-38.
2. Zheng, X. Design and Realization of Pipeline Control System. Nanjing University of Science and Technology, 2013.
3. Wang, Z. Design and Analysis of Underwater Vehicle Electronic Vessel Based on Solidworks and Ansys Workbench. – China High-Tech Enterprise, Vol. **25**, 2014, pp. 1-2.
4. Enshuai, Z. Oil Pipeline Leak Detection and Location Based on Kingview System. – PLC&FA, 2013, No 2, pp. 72-74.
5. Liu, Z. The Study on Auto Tracking Control System for Inspection Robot Used in the Submarine Pipeline. Ocean University of China, 2015.
6. Ji, Z. Application of Underwater Linear Objects Processing Algorithm in Submarin Pipeline Inspection Robot. Ocean University of China. 2015.
7. Jiang, M. Research on Image Binarization Technique. – Software Guide, Vol. **8**, 2009, No 4, pp. 176-177.
8. Jia, G. Binarisation Method for Images Acquired under Non-Uniform Illumination. – Computer Applications and Software, Vol. **31**, 2014, No 3, pp. 184-202.
9. Dong, J. Constrastive Analysis of Several Text Image Binarization Methods. – J. North China Univ. of Tech, Vol. **23**, 2011, No 1, pp. 26-32.
10. Qiang, C. Image Binarization Based on Canny's Operator. – Journal of Computer-Aided Design & Computer Graphics, Vol. **17**, 2005, No 6, pp. 1304-1306.
11. Liu, L. Several Methods of Determining Reression Coefficient in Linear Regression Equation. – Journal of Shenyang Normal University (Natural Science Edition), Vol. **26**, 2008, No 4, pp. 407-408.
12. Shi, R. The Study Based on Unitary Regression Analysis. Hebei University of Science and Technology, 2009.
13. Wang, X. Research on Insect Image Segmentation Based on Multiple Linear Regression. Jiangxi University of Science and Technology, 2014.
14. Wang, B. Computation of Center of Mass for Gray Level Image Based on Differential Moment Factor. – Journal of Computer-Aided Design & Computer Graphics, Vol. **16**, 2004, No 10, pp. 1361-1365.

*Received 23.10.2017; Second Version 07.06.2018; Accepted 25.06.2018*